A Flexible and Robust Solution for Automated 384-well HDAC Profiling

Brad Larson, Peter Banks, BioTek Instruments, Inc., Winooski, VT
Diana Hulboy, Kara Cannon, Wayne Patton, Enzo Life Sciences, Farmingdale, NY

KEY WORDS:
Epigenetics
Histone Deacetylase
HDAC
HDAC Selectivity
Gene Regulation
Profiling
Automation
Fluorescence

BioTek Instruments, Inc.
P.O. Box 998, Highland Park,
Winooski, Vermont 05404-0998 USA
Tel: 888-451-5171
Outside the USA: 802-655-4740
E-mail: customercare@biotek.com
www.biotek.com

Histone deacetylases (HDACs) remove acetyl groups from ε-N-acetyl lysine residues on histones and other proteins. Acetyl group removal serves to increase the positive charge of histone tails, thus encouraging binding between histones and the DNA backbone and preventing transcription. HDACs are implicated in many human diseases, including cancer; making them an increasingly popular drug discovery research target. Here we monitor the deacetylation activity of multiple Class I and II HDAC enzymes in an automated fashion. Validation and pharmacology results demonstrate how the fluorescent assay technology and automated instrumentation may be used together to assess enzyme kinetics and inhibition.

Introduction

Histones are proteins that bind with DNA to form a nucleosome core in eukaryotic chromatin, and are important components of gene regulation. Histone N-terminal tails are subject to many post-translational modifications, including phosphorylation, methylation, ubiquitination, ADP-ribosylation and acetylation. These modifications are proposed as constituting a histone code, with profound regulatory functions in gene transcription1. The best-studied modifications, ε-amino acetylations of specific histone lysine residues, are catalyzed by histone acetyltransferases (HATs), correlating with an open and decondensed chromatin structure and gene activation[2-4]. Histone deacetylases (HDACs), correlating with condensed chromatin and transcriptional repression, are responsible for the removal of these acetyl groups[2-7]. Their importance in gene regulation makes HDACs an increasingly accepted cancer therapy target[8-11].

Although HDAC inhibitors reported thus far are structurally diverse, ranging into chemical classes including hydroxamic acid derivatives, benzamides, cyclic peptides, short-chain fatty acids, etc, most of these inhibitors are equally active against HDACs of class I, II, and IV. Only a few inhibitors are class selective among class I and II enzymes; even fewer are member-selective within a specific class[12]. Thus selectivity profiling of hits from HTS should be of paramount importance for any HDAC "Hit to Lead" program.

Here we demonstrate a simple automated solution for performing HDAC selectivity profiling using an automated pipetting station and a fluorescent technology developed for a wide range of HDAC enzymes. The fluorescent assay is based upon a green pro-fluorescent substrate/developer combination. The substrate, which comprises an acetylated lysine side chain, is incubated with the HDAC enzyme. Deacetylation sensitizes the substrate so that treatment with the developer produces a fluorophore. The pipetting station performs compound titrations and dispenses all assay reagents to a 384-well assay plate such that dose response curves can be defined for each hit from HTS against various HDAC enzymes[-8]. We will demonstrate the utility of this system by profiling a series of known HDAC inhibitors against HDAC-3, -6, -8 and [-10].

Material and Methods

Materials

Fluor de Lys®-Green Substrate (catalog # BML-KI572), Fluor de Lys® Developer Concentrate (20X) (catalog # BML-KI105), Trichostatin A (catalog # BMLGR309), and HDAC Assay Buffer II (catalog # BML-KI422) are part of the Fluor de Lys® HDAC2 Fluorimetric Drug Discovery Kit (catalog # BML-AK512), and were donated by Enzo Life Sciences (Farmingdale, New York). Trichostatin A (catalog # BML-GR309), BML-210 (catalog # BML-GR330), Apicidin (catalog # BML-GR340), Scriptaid (catalog # BML-GR326),

Suberoyl bis-hydroxamic acid (catalog # BML-GR323), Tubacin (catalog # BML-GR362), Niltubacin (catalog # BML-GR363), and BML-281 (catalog # BML-GR361) were also attained from Enzo Life Sciences. Compounds were resuspended in 100% DMSO to the correct 200X concentration for use in the pharmacology validation. All experiments used 384-well, flat bottom, black, non-treated plates (catalog # 3710) from Corning Life Sciences (Corning, New York).

The Precision™ Microplate Pipetting System (Winooski, Vermont) was used to serially titrate compounds across a 96-well polypropylene plate, transfer the compounds to 384-well assay plates, and dispense all assay components to the plates.

A Synergy™ H4 Hybrid Multi-Mode Microplate Reader (Winooski, Vermont) used a filter-based fluorescence system and Xenon flash lamp for all readings. Instrument detection components and optimized instrument settings are detailed in Table 1.

Instrument Detection Component	Wavelength (nm)	BioTek Catalog Number
Excitation filter	485/20	7082221
Emission filter	528/20	7082247
Dichroic mirror	510 cut-off	7138510

Optimized Instrument Settings	
Light source	Xenon flash lamp
Delay after plate movement	0 mS
Measurements per data point	20
Lamp energy	High
Top probe vertical offset	7.0 mm

Table 1. Synergy H4 Instrument Settings.

Methods

Fluor de Lys®-Green HDAC Assay Principle

The two-step Fluor de Lys®-Green assay (Figure 1) is based upon the Fluor de Lys®-Green substrate and Fluor de Lys® developer combination. The substrate avoids quenching and fluorescent interference seen in compounds that absorb in the near ultraviolet and blue ranges. First, the Fluor de Lys®-Green substrate, which comprises an acetylated lysine side chain, is incubated with the HDAC enzyme. Deacetylation sensitizes the substrate so that, in the second step, treatment with the Fluor de Lys® Developer produces a fluorophore. The fluorophore is excited at 485 nm (470 - 500) and emits at approximately 530 nm.

Per each assay procedure, the Precision was used to dispense 5 µL of titrated compounds to a microplate along with 5 µL HDAC enzyme and 10 µL Fluor de Lys®-Green substrate. The plates were shaken on an orbital shaker for 30 seconds at 1000 RPM, and incubated for 60 minutes at room temperature. Following incubation, 20 µL Fluor de Lys® Developer was added to the plates using the Precision, and the plates were again shaken on an orbital shaker for 30 seconds at 1000 RPM and incubated for 20 minutes at room temperature. The plates were then read on the Synergy H4 using the aforementioned optimized instrument settings.

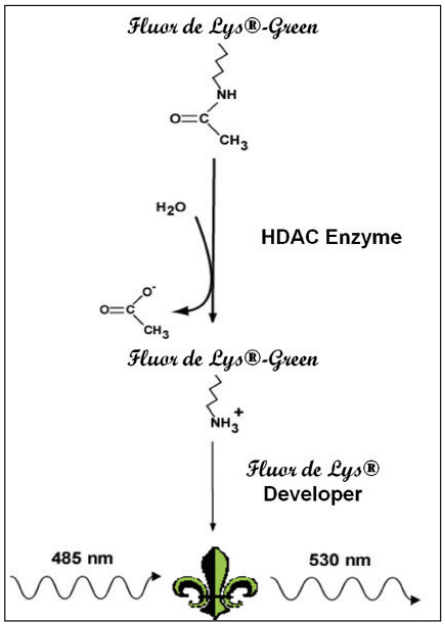

Figure 1.

Data Reduction

The delta RFU value for each well was calculated using the following formula:

$$\Delta \text{ RFU} = (\text{Sample}_{\text{Enz}} - \text{Sample}_{\text{NoEnz}})$$

Where $\text{Sample}_{\text{Enz}}$ are assay wells containing enzyme, substrate, and developer, and $\text{Sample}_{\text{NoEnz}}$ are control wells containing substrate, developer and no enzyme. The measure of a sample's deacetylation is the difference between its fluorescence and the fluorescence of the no enzyme control.

HDAC Enzyme Titration

An enzyme titration demonstrated the ability of the HDAC enzymes to function correctly with the Fluor de Lys®-Green assay. Enzymes were serially titrated using a 1:2 dilution, and then added to the assay plate in triplicate. Fluor de Lys®-Green substrate was then added at a 2X concentration of 20 µM, and the assay plate was incubated per the aforementioned assay procedures. Fluor de Lys® Developer was then added to stop the reaction, the plate was incubated again, and read on the Synergy H4.

Fluor de Lys®-Green Substrate Deacetylation Kinetics

Fluor de Lys®-Green substrate was titrated to determine the substrate Km with each HDAC enzyme. The substrate was serially titrated using a 1:2 dilution, creating final 1X concentrations ranging from 1000-0 µM. Then, 25 ng/well HDAC3, 25 ng/well HDAC6, 0.03 ng/well HDAC8, and 12.5 ng/well HDAC10 were added to each respective assay plate. Triplicate titrated substrate was then added to each assay plate, and the plates were incubated per the aforementioned assay procedures. Fluor de Lys® Developer substrate was added to each, and the plates were incubated again, and read on the Synergy™ H4.

HDAC Enzyme Activity Confirmation

Confirmation of HDAC activity was performed using multiple concentrations of each enzyme. Fluor de Lys®-Green substrate concentrations of 100, 50, 35, and 20 µM were chosen for HDAC3, HDAC6, HDAC8, and HDAC10, respectively, to be below the determined substrate Km. All other assay parameters were as previously described.

Automated HDAC Assay Z'-factor Validation

A Z'-factor assay was performed to validate the HDAC assays using optimized enzyme and substrate conditions. Forty-eight replicates of a positive control including enzyme, and a negative control with no enzyme, were tested. All other assay parameters were as previously described.

HDAC Inhibitor Pharmacology Validation

Inhibitor dose response curves were generated using Trichostatin A, Scriptaid, Apicidin, bis-hydroxamic acid, and BML-210. Also included were the HDAC6 specific inhibitors BML-281 and Tubacin; and Niltubacin was the inactive control. All inhibitors were tested with each enzyme to determine the inhibitor specificity for each enzyme.

Results and Discussion

HDAC Enzyme Titration

Determining the response of an assay chemistry with a particular enzyme is critical before optimization experiments are performed. The enzyme must be able to deacetylate the Fluor de Lys®-Green substrate for the assay to generate the appropriate data. The HDAC enzyme titration curve results (Figure 2) demonstrate proper enzyme-substrate interaction, as well as fluorescent response linearity across a wide range of enzyme concentrations. Dashed lines show the enzyme concentration chosen to perform the substrate Km determination.

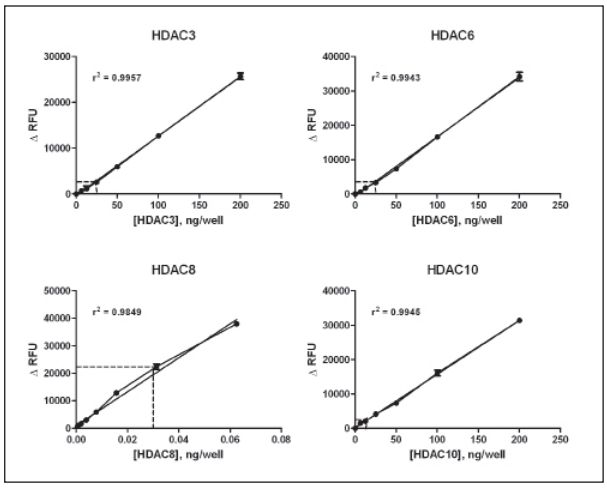

Figure 2.

Fluor de Lys®-Green Substrate Deacetylation Kinetics

Assay sensitivity is improved by using a substrate concentration that is at the Km value for the substrate for that particular enzyme. Using concentrations that are either above or below the Km value can cause compounds to appear more or less potent, respectively, than what they actually are. This is an important consideration for profiling applications. Kinetic data in Figure 3 demonstrate a fluorescence increase in relation to substrate concentration changes. Curves in the left column were calculated using the Michaelis- Menten equation:

$$V=V_{max}[S]/Km+[S]$$

Where V is the reaction rate, Vmax is the maximum conversion rate, [S] is the substrate concentration, and Km is the Michaelis constant.

The Δ RFU vs. Fluor de Lys®-Green curve is slightly sigmoidal, therefore, the determined Km value does not completely fit the data and is right shifted. Data were then fitted to sigmoidal dose-response curves, shown in the right column, for an improved data fit and truer Km value.

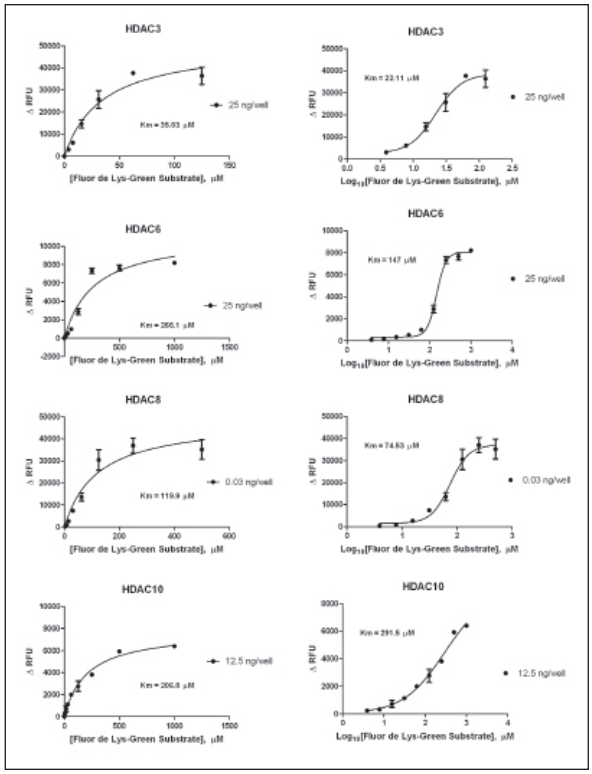

Figure 3.

HDAC Enzyme Activity Confirmation

Once substrate Km values are established, appropriate enzyme concentrations need to be determined. This is typically a balance of minimizing enzyme consumption (i.e. cost) and obtaining sufficient signal relative to background for adequate performance in profiling experiments. It is also important to be certain that the enzyme concentration chosen remains within the initial linear reaction rate, to maintain proper kinetics. A concentration that is not within the linear range would right shift IC_{50} values of compounds tested with that assay. Figure 4 results show that 15, 35, 0.03, and 50 ng/well concentrations yield a significant fluorescence change for HDAC3, HDAC 6, HDAC 8, and HDAC 10, while still within the curve's linear range. This was further demonstrated using a Z'-factor test to determine the assay robustness using the optimized conditions.

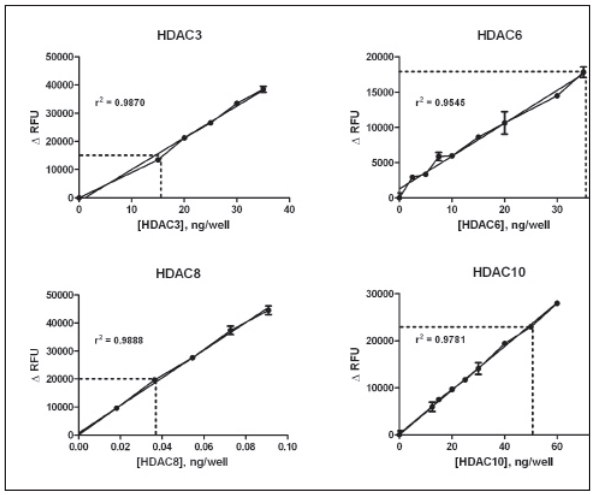

Figure 4.

Automated HDAC Assay Z'-factor Validation

Determining Z'-factor as a statistical parameter has been commonly considered an indicator of robustness of assay performance. It incorporates not only assay and background signals, but also the variability in each. Z'- factor results for each assay (Figure 5) show a Z' value ≥ 0.5. Dashed lines represent the average of three standard deviations for each condition. The calculated Z' values are indicative of excellent assays[13].

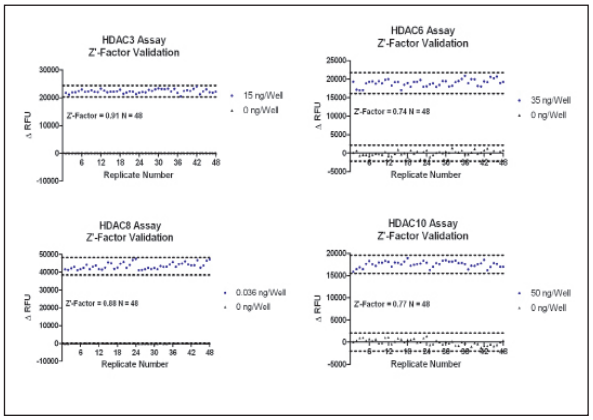

Figure 5.

HDAC Inhibitor Pharmacology Validation

In order to critically evaluate the performance of the automated assay, compound profiling experiments using known inhibitors of the included HDAC enzymes were performed. Inhibitor dose response curves were generated, where nine compounds were each profiled against HDAC3, HDAC 6, HDAC 8, and HDAC 10. Per Figure 6a, it is clear that the enzymes tested provide varying levels of inhibition. These curves are representative of typical data, and were also used to calculate IC_{50} values. Additionally, per the BML-281 and Tubacin inhibition curves in Figure 6b, it is clear that these two compounds are selective, potent inhibitors of HDAC6.

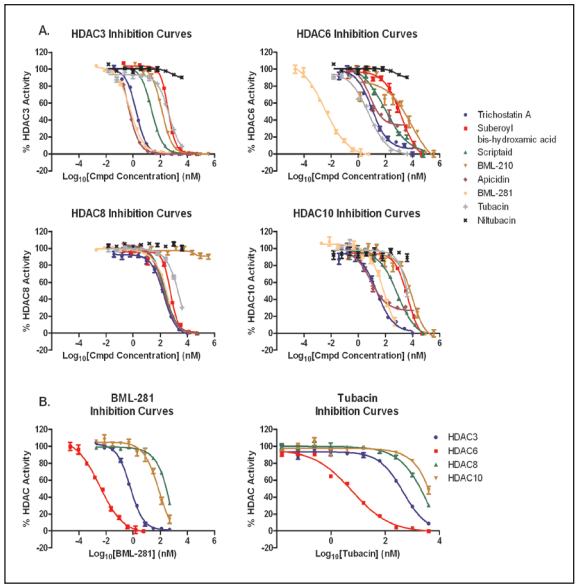

Figure 6.

IC_{50} values per Table 2 were calculated using Prism Software, version 5.01, from GraphPad Software (La Jolla, California). BML-281 and Tubacin IC_{50} values generated from HDAC6 curves compare favorably to published IC_{50} values or internal IC_{50} values generated by the manufacturer.

	BML-281		Tubacin	
	Literature IC_{50} Value	Fluor de Lys®-Green HDAC Assay	Literature IC_{50} Value	Fluor de Lys®-Green HDAC Assay
HDAC3	0.42 nM[1]	0.61 nM	~4000 nM[3]	450.1 nM
HDAC6	0.002 nM[2]	0.003 nM	4 nM[4]	5.9 nM
HDAC8	5-10 µM[1]	>500 nM	~4000 nM[3]	>4000 µM
HDAC10	90.7 nM[1]	86.94 nM	~4000 nM[3]	>4000 nM

[1]Enzo Life Sciences Internal Unpublished Results; [2]Kozikowski et al., 2008
[3]Butler *et al*., 2010; [4]Wong *et al*., 2003

Table 2.

References

1. Strahl, B.D.; Allis, C.D. The language of covalent histone modifications. Nature. 2000, 403(6765), 41-45.

2. Kadosh, D.; Struhl, K. Targeted recruitment of the Sin3-Rpd3 histone deacetylase complex generates a highly localized domain of repressed chromatin in vivo. Mol Cell Biol. 1998, 18(9), 5121-5127.

3. Rundlett, S.E.; Carmen, A.A.; Suka, N.; Turner, B.M.; Grunstein, M. Transcriptional repression by UME6 involves deacetylation of lysine 5 of histone H4 by RPD3. Nature. 1998, 392(6678), 831-835.

4. Zhang, Y.; Sun, Z.W.; Iratni, R.; Erdjument-Bromage, H.; Tempst, P.; Hampsey, M.; Reinberg, D. SAP30, a novel protein conserved between human and yeast, is a component of a histone deacetylase complex. Mol Cell 1998, 1(7), 1021-1031.

5. Grunstein, M. Histone acetylation in chromatin structure and transcription. Nature. 1997, 389(6649), 349-352.

6. Ng, H.H.; Bird, A. Histone deacetylases: silencers for hire. Trends Biochem Sci. 2000, 25(3), 121-126.

7. Cheung, W.L.; Briggs, S.D.; Allis, C.D. Acetylation and chromosomal functions. Curr Opin Cell Biol. 2000, 12(3), 326- 333.

8. Marks, P.A.; Miller, T.; Richon, V.M. Histone deacetylases. Curr Opin Pharmacol. 2003 Aug, 3(4), 344-351.

9. Marcus, A.I.; Zhou, J.; O'Brate, A.; Hamel, E.; Wong, J.; Nivens, M.; El-Naggar, A.; Yao, T.P.; Khuri, F.R.; Giannakakou, P. The synergistic combination of the farnesyl transferase inhibitor lonafarnib and paclitaxel enhances tubulin acetylation and requires a functional tubulin deacetylase. Cancer Res. 2005 May 1, 65(9), 3883-3893.

10. Saji, S.; Kawakami, M.; Hayashi, S.; Yoshida, N.; Hirose, M.; Horiguchi, S.; Itoh, A.; Funata, N.; Schreiber, S.L.; Yoshida, M.; Toi, M. Significance of HDAC6 regulation via estrogen signaling for cell motility and prognosis in estrogen receptor-positive breast cancer. Oncogene. 2005 Jun 30, 24(28), 4531- 4539.

11. Carew, J.S.; Giles, F.J.; Nawrocki, S.T. Histone deacetylase inhibitors: mechanisms of cell death and promise in combination cancer therapy. Cancer Lett. 2008 Sep 28. 269(1), 7-17.

12. Su, H; Atucci, L; Yon, Q. Competitive or non competitive, that's the question: research towards histone deacetylase inhibitors. Mol. Canver Ther.. 2008, 7(5), 1007-12.

13. Zhang, J.H.; Chung, T.D.; Oldenburg, K.R. A Simple Statistical Parameter for Use in Evaluation and Validation of High Throughput Screening Assays. J Biomol Screen. 1999, 4(2), 67-73.